Received: Added at production | Revised: Added at production | Accepted: Added at production
DOI: xxx/xxxx

RESEARCH ARTICLE

Engineering Reports
Open Access

Development and Error Analysis of 3D Laser Tracking Ball Bar

Ying-zhi Zhang[1] | Gong-chang Ren*[2] | Hai-tao Li[3]

College of mechanical & electrical engineering, Shaanxi University of Science and Technology, Xi'an, China

Correspondence
*Gong-chang Ren, College of mechanical & electrical engineering, Shaanxi University of science and technology, Xi'an, 710021, China
Email: 294593600@qq.com

Funding Information
The Project Supported by Natural Science Basic Research Plan in Shaanxi Province of China, Grant/Award Number: 2019JQ-783;
Scientific Research Program Funded by Shaanxi Provincial Education Department, Grant/Award Number: 19JK0138

Abstract

As a high-precision measuring instrument, laser tracker is widely used in the field of geometric error detection of CNC machine tools. However, the employment of this laser tracker will lead to high cost as well as low measurement accuracy caused by the angle error. In order to solve these problems, the passive 3D laser tracking ball bar based on the principle of laser interference is introduced in this paper. The following measurement is realized by the passive stretching of the telescopic mechanism, and the space attitude adjustment of the laser is ensured by two precise rotating shafts. Moreover, the deflection caused by the telescopic guideway is an important factor affecting the accuracy of the device. Therefore, the telescopic mechanism is designed by the maximum deviation of the laser obtained by the experiment, and the finite element analysis is carried out. The results showed that the accuracy requirements are met. The main error model of the device is established and the influence of each error is analyzed. Moreover, the simulation results showed that the vertical axis offset angle error has the greatest impact on the device. At last, the reason of different influence of errors on the device is analyzed.

KEYWORDS

Laser tracker, error modeling, accuracy analysis, telescopic mechanism

1 | INTRODUCTION

As the concentrated embodiment of manufacturing industry, improving the accuracy of machine tools is of great significance [1]. Among all the errors affecting the accuracy of machine tools, geometric errors have the greatest impact, reaching more than 40% [2]. At present, two methods are used to reduce the geometric error of machine tools: error prevention and error compensation [3]. The employment of error prevention can improve the accuracy of key parts of machine tools, but it will greatly increase both the cost and manufacturing difficulty [4]. Through error compensation, all kinds of errors of machine tools can be identified, and then compensated by appropriate mathematical model and algorithm [5]. What's more, error compensation can improve the accuracy of machine tools at low cost, but the question is how to solve the problem of identifying the geometric errors of the CNC machine

Received: Added at production | Revised: Added at production | Accepted: Added at production
DOI: xxx/xxxx

precisely. The identification of geometric error of machine tools has been developed with the updating of detection instruments [6-7]. Laser interferometer has the highest accuracy in measuring geometric errors, but the corresponding optical path needs to be set up before measuring different errors. Besides, the steps are tedious and inefficient [8]. The single station method of laser tracker can identify errors rapidly, but due to the influence of angle error, the measurement accuracy cannot be guaranteed [9]. Wang [10-11] put forward a method of geometric error identification based on time-sharing GPS. In his research, a laser tracker is used to measure the same movement track of CNC machine tools at different stations in order. Based on the principle of GPS, the relative spatial position of the station and the spatial coordinates of each measuring point are determined. Then, based on the principle of nine-line error separation, the geometric errors of the machine tool are separated, but the laser tracker is so expensive that many measurement agencies can't afford it [12]. Therefore, it is necessary to develop an instrument at low cost but with high accuracy.

In order to solve the problems mentioned above, this paper proposes a 3D laser tracking ball bar with simple structure for measuring geometric errors of machine tools. This 3D laser tracking ball bar is designed based on the principle of laser interferometry. The laser attitude is followed passively by two rotating axes, and the distance is followed by telescopic guide rail.

The structure of this paper is as follows. The 3D laser tracking ball bar is described in detail in Chapter 2. In Chapter 3, the error source of the instrument is analyzed and the error model is deduced. Chapter 4 describes the influence degree of each error to the instrument through simulation. Finally, the conclusions are shown in Chapter 5.

2 | STRUCTURAL DESIGN

2.1 | 3D LASER TRACKING BALL BAR

As shown in Figure 1, the 3D laser tracking ball bar consists of two precision rotating shafts and a telescopic mechanism. There are two standard balls for measurement. One is installed at the end of the telescopic mechanism to follow the movement of the spindle, the other is installed under the platform, and the connection between the two ball centers is parallel to the laser. Renishaw XL80 is used to measure the relative distance of the telescopic mechanism. A 3D coordinate system is established as well.

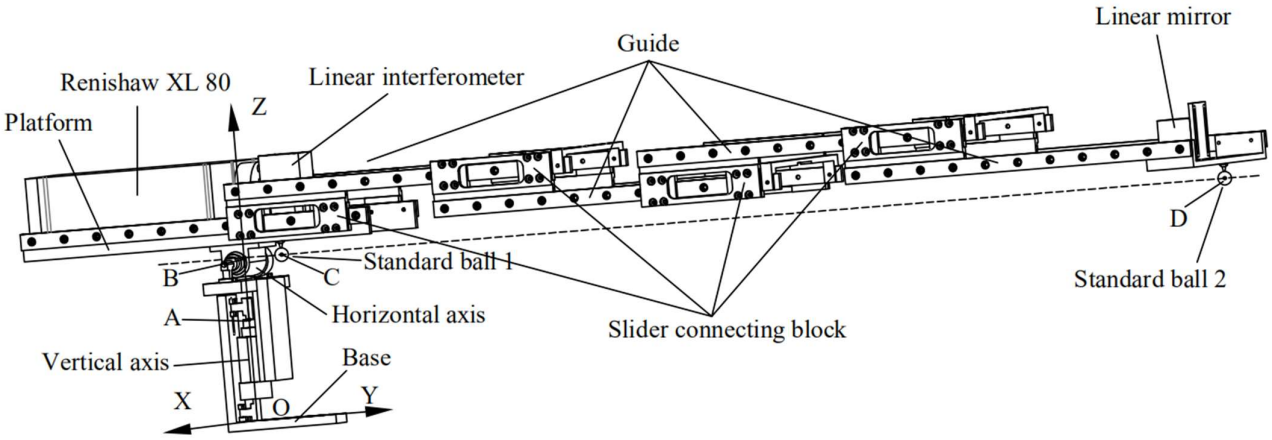

Figure 1 Example of a figure with caption

Received: Added at production | Revised: Added at production | Accepted: Added at production
DOI: xxx/xxxx

2.2 | DESIGN OF TELESCOPIC MECHANISM

As one of the main moving parts of the 3D laser tracking ball bar, the assembly error and stress deformation will seriously affect the movement accuracy of the telescopic mechanism in the cantilever state [13]. Consequently, the accuracy of Renishaw XL80 is seriously affected. When Renishaw XL80 has five green lights, the accuracy level of measurement reaches the highest. In order to ensure the measurement accuracy, at least three lights should be on during the measurement. However, too much offset of the telescopic mechanism interrupts the measurement. Therefore, the maximum deformation of the telescopic mechanism should be smaller than the maximum vertical deviation of allowed by Renishaw XL80. The migration diagram of Renishaw XL80 is shown in Figure 2.

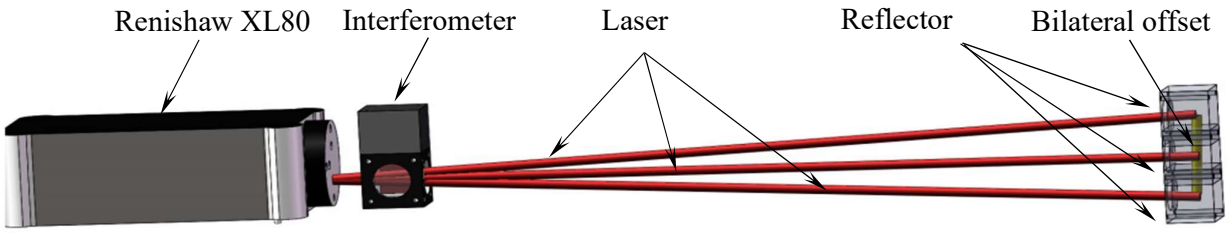

Figure 2 Renishaw xl80 offset diagram

In this section, the vertical offset experiment of Renishaw XL80 is established. The experimental principle is shown in Figure 3. The experimental scheme is as follows.

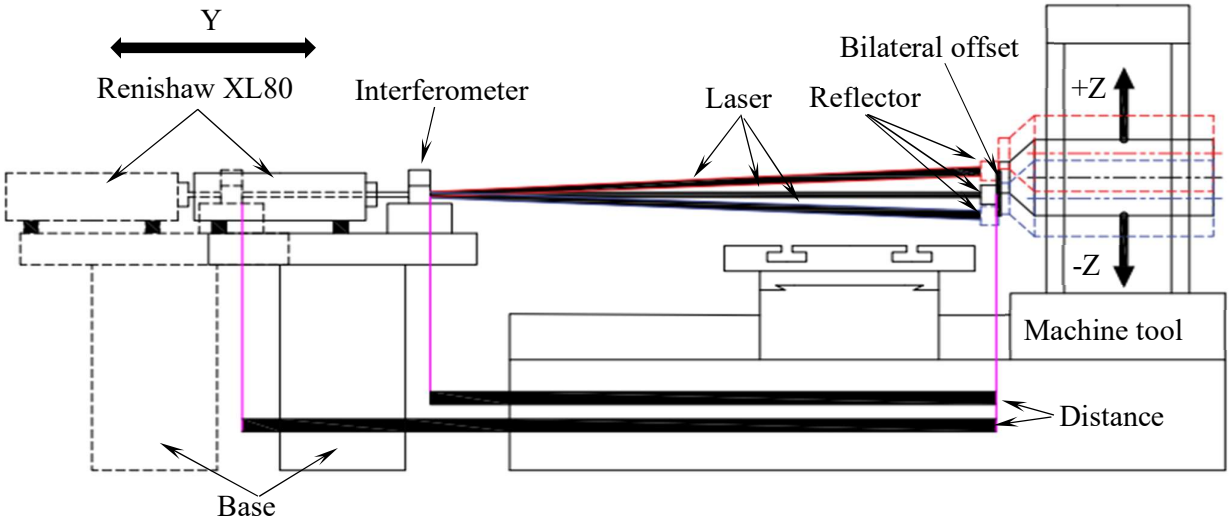

Figure 3 Schematic diagram of Migration Experiment

Received: Added at production | Revised: Added at production | Accepted: Added at production
DOI: xxx/xxxx

A high-precision CNC is used to measure the maximum allowable offset in direction Z of Renishaw XL80 at different measuring distances. The reflector is installed on the spindle of the machine tool, and linear measurement of optical path based on Renishaw XL80 with five lights is set up, then the reciprocating motion on axis Z of the machine tool is controlled, and the maximum bilateral offset allowed by the Renishaw xl80 under different accuracy levels is recorded. The maximum bilateral offset in direction Z allowed by XL80 under four kinds of ranging is obtained. The experiment at three-axis machine tool is shown in Figure 4.

Figure 4 experiment at three-axis machine tool

The measurement data is shown in Table 1.

Table 1 Renishaw xl80 offset under different ranging

Measuring distance	Bilateral offset (mm)				
	5 lights	4 lights	3 lights	2 lights	1 lights
100 cm	1.18	1.512	1.794	2.095	2.61
125 cm	1.10	1.47	1.77	2.07	2.44
150 cm	1.06	1.43	1.74	2.056	2.29
175 cm	1.019	1.391	1.712	2.036	2.15

The curve equation of offset varying with measuring distance is fitted by least square method. Curves are shown in Figure 5. The fitting equation is as follows:

Received: Added at production | Revised: Added at production | Accepted: Added at production
DOI: xxx/xxxx

$$\begin{cases} y_1 = (-0.00104 \pm 1.38564 \times 10^{-4})x + (0.688 \pm 0.01944) \\ y_2 = \left((-8) \times 10^{-4} \pm 1.26491 \times 10^{-5}\right)x + (0.8355 \pm 0.00177) \\ y_3 = ((-5.52 \times 10^{-4} \pm 1.69706 \times 10^{-5})x + (0.9529 \pm 0.00238) \end{cases} \quad (1)$$

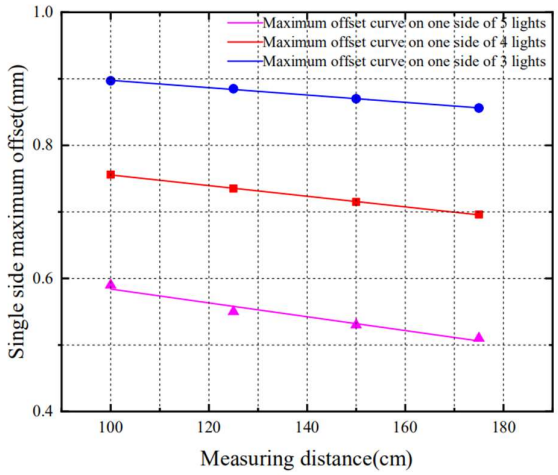

Figure 5 The curve of offset varying with measuring distance

The maximum deviation of the telescopic mechanism is obtained by substituting the expected measurement range of the telescopic mechanism into the equation. The size of the telescopic guide is 800mm, and the maximum deviation is 0.0035, 0.1955, and 0.5113, respectively.

Based on the parameter, the telescopic mechanism is designed and its structure is shown in the Fig. 6. The slide motion unit of the guide rail is used as the basic component of the single telescopic guide. The telescopic motion function is realized through the stack installation of the slide motion unit of the guide rail. The unilateral telescopic guide is symmetrically installed on both sides of the interferometer platform, the end of which is fixed on both sides of the reflector platform, thus forming the overall structure of the telescopic mechanism.

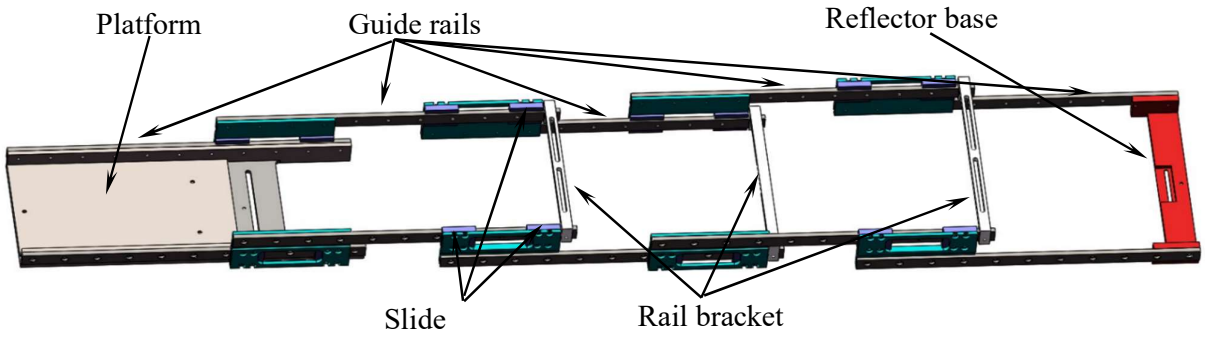

Figure 6 The structure of telescopic guide

2.3 | FINITE ELEMENT ANALYSIS OF EXPANSION DEVICE

In this section, the finite element simulation of the telescopic mechanism is carried out to obtain the deflection deformation of the telescopic mechanism in the cantilever state. The material properties of each part are shown in Table 2.

Received: Added at production | Revised: Added at production | Accepted: Added at production
DOI: xxx/xxxx

Table 2 Material details

Part	Material	Density (kg/m^3)	Modulus of elasticity ($10^{10}pa$)	Poisson's ratio
Slide	6061-T6	1804	70	0.33
Rail bracket	6061-T6	1804	70	0.33
Reflect base	Q235	7850	2	0.3
Renishaw xl80	Q235	7850	2	0.3
Platform	Q235	7850	2	0.3

The pressure applied by each part is simplified into three forces. The forces are shown in Figure 7, where $F_1 = 16.53N$, $F_2 = 18.5N$, $F_3 = 13.235N$. The mesh is divided by ANSYS, the boundary conditions and load are set, and the equivalent stress is added to the navigation tree, then the solution is carried out, and the total deformation cloud diagram is shown in Figure 8.

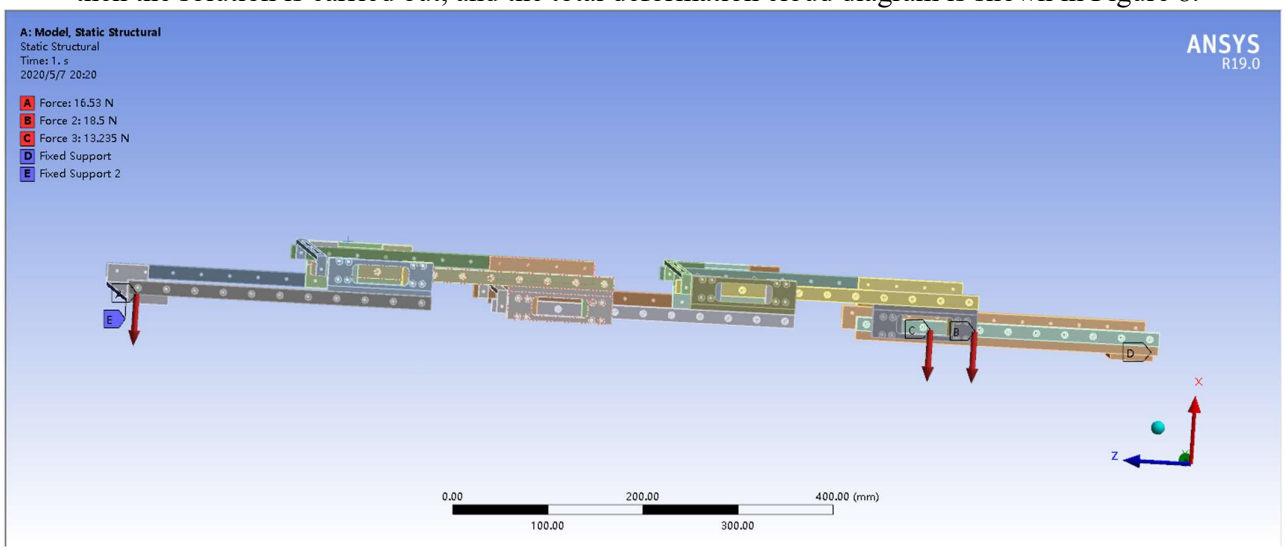

Figure 7 Structural of telescopic guide

It can be seen from Figure 8 that the maximum deformation of the telescopic mechanism under the set boundary condition is 0.02729mm, which is obviously smaller than the allowable maximum deviation data in Section 2.2. Therefore, it can be inferred that the telescopic mechanism has strong resistance to deformation, and micro deformation does not affect the measurement accuracy. What's more, the telescopic mechanism can ensure the uninterrupted laser during the measurement.

Received: Added at production | Revised: Added at production | Accepted: Added at production
DOI: xxx/xxxx

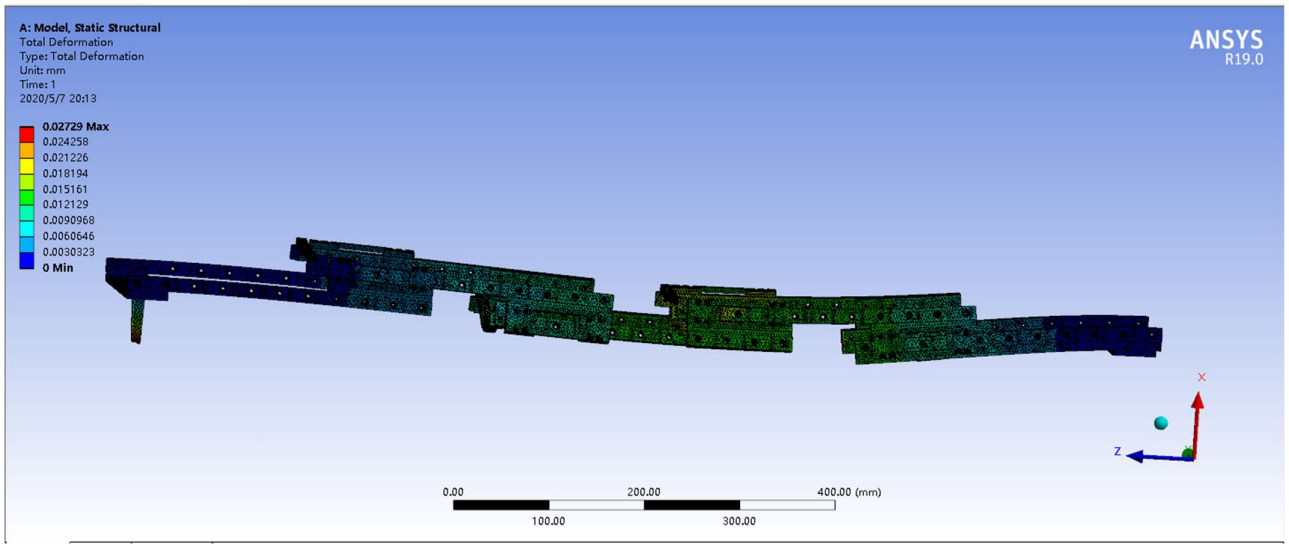

Figure 8 Structural of telescopic guide

Chapter 2 first introduced the structure of 3D laser tracking ball bar and the establishment of the coordinate system. Then the design of the telescopic mechanism was introduced. It has a great impact on the accuracy of the device in detail, including the experiment of the maximum offset of the telescopic mechanism, the design of the telescopic mechanism. Finally, through the finite element simulation, the telescopic mechanism is verified to meet the measurement accuracy requirements.

3 | MAIN ERROR ANALYSIS

In this chapter, the main errors of the 3D laser tracking ball bar are analyzed. Firstly, the model is simplified and the error sources are analyzed. Next, the main errors affecting the accuracy of the device are listed. After that, the mathematical model of each error is established by analytic method, and the position of the device affected by each error is analyzed.

3.1 | THE MAIN ERROR OF THE 3D LASER TRACKING BALL BAR

Fig.9 shows the coordinate system and the simplified structure model. The measurement of the spatial position can be described as follows. The vertical axis is simplified as the connection between point O and A. The line between Point A and Center O on the vertical axis coincides with Z axis. The line between Point B which is the midpoint of the horizontal axis and point A coincides with the Z axis, and the horizontal axis is parallel to the X axis in the XOY. Point C and D are the centers of standard ball 1 and 2. The line between B and D is parallel to axis Y in YOZ.

L_1: Distance between vertical axis and horizontal axis,

L_2: Distance between standard ball 1 and the midpoint of horizontal axis，

R_L: Measuring distance with laser interferometer,

Z_1: Distance from point A to axis Y.

L_h: Length of horizontal axis

Received: Added at production | Revised: Added at production | Accepted: Added at production
DOI: xxx/xxxx

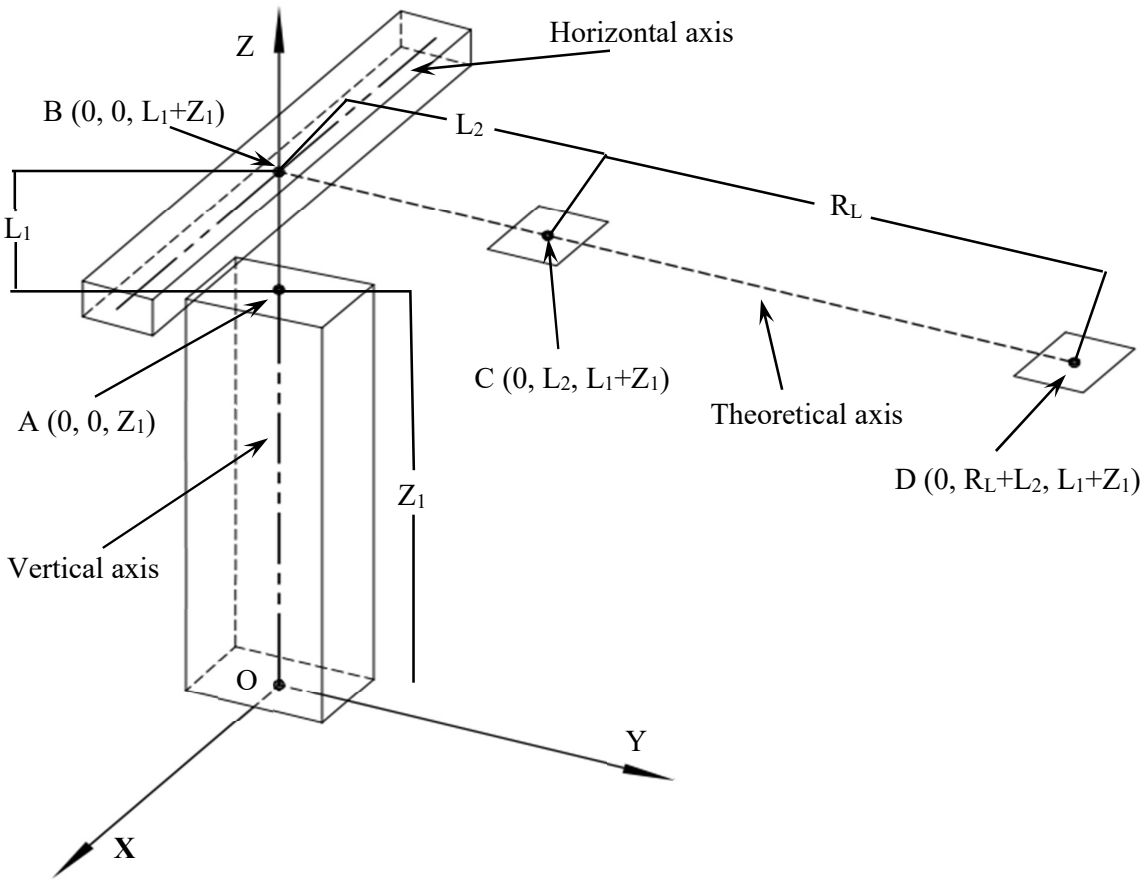

Figure 9 simplified model of 3D laser tracker ball bar

According to the simplified model, the main sources of the error come from the machining error and the assembly error of the parts. Fig. 10 shows the error based on the analysis of the main error sources of the device. The non-coincidence between the vertical axis and axis Z is defined as α and θ. The non-orthogonality between the horizontal axis and the vertical axis is defined as β and γ. The non-coincidence error between the line of two standard spherical centers and the laser light is defined as ω.

Received: Added at production | Revised: Added at production | Accepted: Added at production
DOI: xxx/xxxx

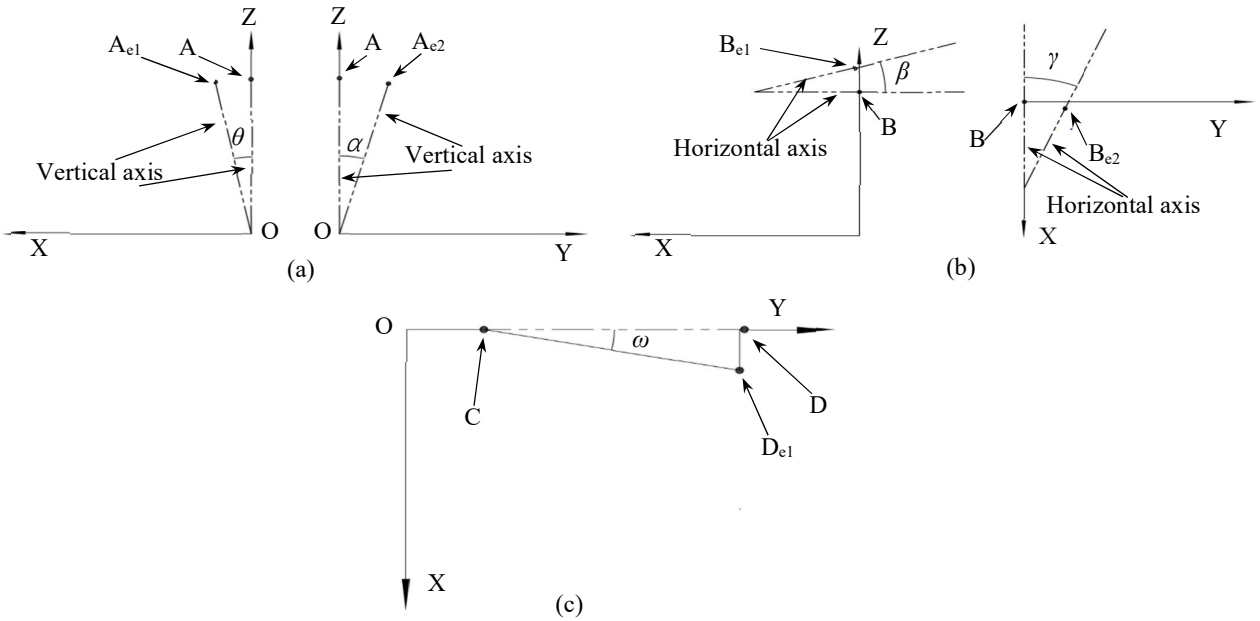

Figure 10 The main error in 3D laser tracker ball bar instrument. (a), error of vertical axis. (b), error of horizontal axis. (c), error of stranded balls

3.2 | ERROR MODEL

The device model without error can be regarded as a point moving in space, starting from point O which moves along the axis Z to point A, then to point B, and down to the axis Y parallel direction to the end point D via point C successively. Any of the above errors have an impact on the accuracy of the device, mainly reflecting in the coordinate offset of point D. Therefore, in this section, the mathematical models of the above errors are established respectively by analytic method. The effect of each error on the device is mathematically modeled by analytic method respectively, which is mainly reflected in the influence of the error on the point D.

As shown in Fig.10 (a), due to the errors θ and α, point A is shifted to A_{e1} and A_{e2}, and the coordinates after migration are as follows:

$$A_{e1} = \begin{cases} x_{e1} = (Z_1 + L_1) \times sin\theta \\ y_{e1} = 0 \\ z_{e1} = (Z_1 + L_1) \times cos\theta \end{cases} \tag{2}$$

$$A_{e2} = \begin{cases} x_{e2} = 0 \\ y_{e2} = (Z_1 + L_1) \times sin\alpha \\ z_{e2} = (Z_1 + L_1) \times cos\alpha \end{cases} \tag{3}$$

The 3D laser tracking ball bar is assembled by various parts, and the assembly and manufacturing errors of parts are transitive. Therefore, the vertical axis error not only changes the point A, but also causes the correlation error of D to shift to D_{e1} or D_{e2}. D_{e1} and D_{e2} can be expressed as:

Received: Added at production | Revised: Added at production | Accepted: Added at production
DOI: xxx/xxxx

$$D_{e1} = \begin{cases} X_{e1} = (Z_1 + L_1) \times sin\theta \\ Y_{e1} = L_2 + R_L \\ Z_{e1} = (Z_1 + L_1) \times cos\theta \end{cases} \tag{4}$$

$$D_{e2} = \begin{cases} X_{e2} = 0 \\ Y_{e2} = \sqrt{(Z_1 + L_1)^2 + (L_2 + R_L)^2} \times \cos\left(90° - \arctan\left(\frac{L_2+R_L}{Z_1+L_1}\right) - \alpha\right) \\ Z_{e2} = \sqrt{(Z_1 + L_1)^2 + (L_2 + R_L)^2} \times \sin\left(90° - \arctan\left(\frac{L_2+R_L}{Z_1+L_1}\right) - \alpha\right) \end{cases} \tag{5}$$

Here, De1 and De2 indicates that θ affects the accuracy of the device in direction X and Z, and α affects the accuracy of the device in direction Y and Z.

In the same way, β and γ in the horizontal axis also cause point B to shift to B_{e1} and B_{e2}. The offset coordinates are as follows:

$$B_{e3} = \begin{cases} x_{e3} = \frac{1}{2}L_h \times (1 - cos\beta) \\ y_{e3} = 0 \\ z_{e3} = L_1 + Z_1 + \frac{1}{2}L_h \times sin\beta \end{cases} \tag{6}$$

$$B_{e4} = \begin{cases} x_{e4} = \frac{1}{2}L_h \times (1 - cos\gamma) \\ y_{e4} = \frac{1}{2}L_h \times sin\gamma \\ z_{e3} = L_1 + Z_1 \end{cases} \tag{7}$$

D_{e3} and D_{e4} caused by horizontal axis errors are as follows:

$$D_{e3} = \begin{cases} X_{e3} = \frac{1}{2}L_h \times (1 - cos\beta) \\ Y_{e3} = L_2 + R_L \\ Z_{e3} = \frac{1}{2}L_h \times (1 - cos\beta) \end{cases} \tag{8}$$

$$D_{e4} = \begin{cases} X_{e4} = \frac{1}{2}L_h - \sqrt{\left(\frac{1}{2}L_h\right)^2 + (L_2 + R_L)^2} \times \sin\left(90° - \gamma - \arctan\left(\frac{2(L_2+R_L)}{L_h}\right)\right) \\ Y_{e4} = \sqrt{\left(\frac{1}{2}L_h\right)^2 + (L_2 + R_L)^2} \times \cos\left(90° - \gamma - \arctan\left(\frac{2(L_2+R_L)}{L_h}\right)\right) \\ Z_{e4} = L_1 + Z_1 \end{cases} \tag{9}$$

From De3 and De4 above, it can be seen that β affects the accuracy in direction X and Z of the device, and γ affects the accuracy in direction X and Y of the device.

The line between the laser light and the two spherical centers is not parallel due to the ω, which makes the measured object deviate from the distance between the two spherical centers, and D_{e5} coordinates are as follows:

Received: Added at production | Revised: Added at production | Accepted: Added at production
DOI: xxx/xxxx

$$D_{e5} = \begin{cases} X_{e5} = R_L sin\omega \\ Y_{e5} = L_2 + R_L cos\omega \\ Z_{e5} = Z_1 + L_1 \end{cases} \quad (10)$$

From Eqs 10, it can be obviously seen that ω affects the accuracy of the device in directions X and Y.

The main errors affecting the accuracy of the device are listed, and the influence of all errors on the device has been derived. The results are shown in Table 3.

Table 3 error influence distribution

In terms of impact	Error
Direction X	ω, γ, β, θ
Direction Y	γ, α
Direction Z	β, α, θ

It can be seen from Table 3 that the 3D laser tracking ball bar is most likely to produce offset in direction X, followed by direction Z, with the least possibility of error in direction Y.

4 | SIMULATION

The mathematical model of deviation caused by various errors has been deduced previously. Any kind of errors that mentioned in Chapter 3 will lead to the deviation of point D, so the degree of deviation of point D is used to measure the degree of error. In order to verify the influence of various errors on the accuracy of the device, the simulation of error model was carried out as follows.

4.1 | 4.1 ERROR SIMULATION

The 3D laser tracking ball bar is simplified to four points as shown in Figure 8, and the theoretical coordinates are as follows respectively: A (0,0,100), B (0,0,145), C (0,35,145), D (0,900,145). Due to the error of the axis in the process of machining or assembling, the actual coordinate is different from the theoretical coordinate. Furthermore, the structural errors are all angle errors, so the simulation will compare the degree of the deviation of point D caused by each error under the same error value. The same values of five angular errors are given three times, which are 0.02, 0.04, and 0.06 respectively. The error simulation results of each direction are shown in Table 4 to Table 6

Table 4 The values of each error in direction X through simulation

Error value(mm)	Error types				
	θ_x	α_x	β_x	γ_x	ω_x
0.02	-0.050	0	$-2*10^{-6}$	-0.314	-0.302
0.04	-0.101	0	$-9*10^{-6}$	-0.628	-0.604
0.06	-0.152	0	$-2*10^{-5}$	-0.942	-0.906

Table 5 The values of each error in direction Y through simulation

Received: Added at production | Revised: Added at production | Accepted: Added at production
DOI: xxx/xxxx

Error value(mm)	Error types				
	θ_y	α_y	β_y	γ_y	ω_y
0.02	0	-0.051	0	-0.014	$5.2*10^{-5}$
0.04	0	-0.011	0	-0.028	$2.1*10^{-4}$
0.06	0	-0.152	0^5	-0.041	$4.7*10^{-4}$

Table 6 The values of each error in direction Z through simulation

Error value(mm)	Error types				
	θ_z	α_z	β_z	γ_z	ω_z
0.02	$8.8*10^{-6}$	-0.314	-0.014	0	0
0.04	$3.5*10^{-5}$	-0.628	-0.027	0	0
0.06	$8.0*10^{-5}$	-0.942	-0.042	0	0

As is shown in Table 4-6, the deviation of point D caused by α and γ is larger, and the deviation caused by θ and β is smaller. Among them, γ causes the maximum deviation in direction X, and α causes the maximum deviation in direction Y and Z. Therefore, when processing and assembling the parts needed for 3D laser tracking ball bar, attention should be paid to the assembly accuracy of the vertical axis in YOZ and the horizontal axis in XOY. Meanwhile, with the increase of angle error, the deviation of the device increases gradually.

4.2 | ERROR INFLUENCE DEGREE

From 4.1 (Error Simulation), it can be seen that α and γ have a greater impact on the accuracy of the device, while θ and β have smaller impact on the accuracy of the device. Therefore, it is necessary to analyze the error model to find out the causes for different degrees of error influence, and the compensation model of each error can be obtained from Section 3.2, as follows:

$$\theta = \begin{cases} \arcsin\left(\frac{X_{e1}}{Z_1+L_1}\right) \\ \arccos\left(\frac{Z_{e1}}{Z_1+L_1}\right) \end{cases} \tag{11}$$

$$\alpha = \begin{cases} \arctan\left(\frac{L_2+R_L}{Z_1+L_1}\right) - \arcsin\left(Y_{e2} - \sqrt{(Z_1+L_1)^2+(L_2+R_L)^2}\right) \\ \arctan\left(\frac{L_2+R_L}{Z_1+L_1}\right) - \arccos\left(Z_{e2} - \sqrt{(Z_1+L_1)^2+(L_2+R_L)^2}\right) \end{cases} \tag{12}$$

$$\beta = \begin{cases} \arccos\left(1 - \frac{2X_{e3}}{L_h}\right) \\ \arcsin\left(\frac{2(Z_{e3}-Z_1-L_1)}{L_h}\right) \end{cases} \tag{13}$$

Received: Added at production | Revised: Added at production | Accepted: Added at production
DOI: xxx/xxxx

$$\gamma = \begin{cases} \arccos\left(\frac{\frac{1}{2}L_h - X_{e4}}{\sqrt{\left(\frac{1}{2}L_h\right)^2 + (L_2+R_L)^2}}\right) - \arctan\left(\frac{2(L_2+R_L)}{L_h}\right) \\ arcsin\left(\frac{\frac{1}{2}L_h - X_{e4}}{\sqrt{\left(\frac{1}{2}L_h\right)^2 + (L_2+R_L)^2}}\right) - \arctan\left(\frac{2(L_2+R_L)}{L_h}\right) \end{cases} \tag{14}$$

$$\omega = \begin{cases} \arcsin\left(\frac{X_{e5}}{R_L}\right) \\ arcsin\left(\frac{Y_{e5}}{L_2+R_L}\right) \end{cases} \tag{15}$$

The five kinds of errors are all transitive. Through the error compensation model, it can be seen that the deviation generated by α, γ and ω are mainly transmitted by R_L, while the deviation of θ and β are mainly transmitted by Z_1. It is known that R_L is far greater than Z_1, the transmitted error also increases with the increase of the associated size, so α and γ have greater impact on the accuracy of the device.

In this chapter, according to the numerical simulation of each errors, it is concluded that the α and γ are the main factors affecting the accuracy of the device. And then through the analysis of the error compensation model, the reasons of the different degree of error influence are found. In conclusion, this chapter provides the theoretical basis of error compensation and assembly requirements.

5 | CONCLUSION

In this paper, the 3D laser tracking ball bar for measuring geometric errors of CNC machine tools is proposed and its structure is designed. Then the accuracy of the telescopic mechanism is verified. Based on the analysis of the error sources, the main errors that affect the measurement accuracy of the device are analyzed. Furthermore, the error model is established, and the influence degree of the errors is analyzed through simulation so as to facilitate the compensation of the instrument error. The main conclusions are as follows:

(1) After analyzing the advantages and disadvantages of the existing geometric error measurement methods of machine tools, a more economical 3D laser tracking ball bar is proposed and the coordinate system is established. The device ensures the attitude following with two rotating axes, and the telescopic device ensures the distance following. As the telescopic device is the main factor affecting the measurement accuracy, Chapter 2 focuses on the design of the telescopic device. The maximum vertical deviation of Renishaw xl80 under different distances is measured by the maximum deviation experiment, and the maximum deviation curve is fitted by the least square method. The maximum allowable offsets under three accuracy conditions are 0.0035, 0.1955 and 0.5113mm respectively. After the finite element analysis of the telescopic device, the result shows that the vertical offset is 0.0024mm, which meets the measurement accuracy requirements.

(2) Based on the analysis of error sources, five errors affecting the accuracy of the device are discovered, and error models are established one by one. According to the error model, four errors affect the accuracy in direction X, namely, ω, γ, β and θ. Two errors affect the accuracy of direction Y, including γ and α. The accuracy of direction Z is affected by another three errors, namely β, α, θ. After that, through the numerical simulation by MATLAB, the results show

that α γ and ω have greater impact on the accuracy of the device. The reasons are as follows: these three errors are transmitted through measuring distance with Renishaw xl80, and the distance is the largest, so that the error is amplified through R_L, leading to the greater impact on the accuracy of the device. The error analysis above provides the theoretical basis for the error compensation of the 3D laser tracking ball bar and assembly requirements.

ACKNOWLEDGEMENTS

The authors are grateful for the financial support from Department of science and technology of Shaanxi Province (Grant 2019JQ-783)and Department of education of Shaanxi Province (Grant 19JK0138) .

CONFLICT OF INTEREST

Authors have no conflict of interest relevant to this article.

REFERENCES

[1] Schwenke H., Knapp W, Haitjema H, et al. Geometric error measurement and compensation of machines-An update. *CIRP Annals-Manufacturing Technology*, 2008, 57(2):660-675.

[2] Ramesh R, Mannan M A, Poo A N, et al. Error compensation in machine tools-a review Part I: Geometric, cutting-force induced and fixture-dependent errors. *International Journal of Machine Tools & Manufacture*, 2000, 40(9):1235-1256.

[3] Sartoria S, Zhang GX. Geometric Error Measurement and Compensation of Machines, *CIRP Annals – Manufacturing Technology*,1995, 44(2):599-609.

[4] Alessandro Velenosi, Gianni Campatelli, Antonio Scippa. Axis geometrical errors analysis through a performance test to evaluate kinematic error in a five axis tilting-rotary table machine tool. *Precis Eng* 2015;39:224–33.

[5] SCHWENKE H, FRANK M, HANNAFORD J. Error mapping of CMMs and machine tools by a single tracking interferometer. *CIRP Annals-Manufacturing Technology*, 2005, 54(1): 475-478.

[6] Zhou Yuansheng, Chen Zezhong C, Yang Xujing. An accurate, efficient envelopeapproach to modeling the geometric deviation of the machined surface for a specific five-axis CNC machine tool. *Int J Mach Tools Manuf* 2015;95:67–77.

[7] S. Wang, B. Zhou, C. Fang, S. Sun, Research on thermal deformation of large CNC gear profifile grinding machine tools, *Int. J. Adv. Manuf. Tech* 91 (2016) 577–587.

[8] Cui G W, Lu J, Gu Y F, et al. Research on Real-time Synthetic Error Compensation Principle for CNC machine Tool. *Advanced Materials Research*, 2011, 314-316: 2454-2457.

Received: Added at production | Revised: Added at production | Accepted: Added at production
DOI: xxx/xxxx

[9] S. Wang, B. Zhou, C. Fang, S. Sun, Research on thermal deformation of large CNC gear profifile grinding machine tools, *Int. J. Adv. Manuf. Tech* 91 (2016) 577–587.

[10] Wang Jindong, Guo Junjie, Zhou Baoqing, Xiao Jian. The detection of rotary axis of NC machine tool based on multi-station and time-sharing measurement. *Measurement*, 2012, 45:1713-1722.

[11] Wang Jindong, Guo Junjie, Zhang Guoxiong, Guo Bao'an, Wang Hongjian. The technical method of geometric error measurement for multi-axis NC machine tool by laser tracker. *Measurement Science and Technology*, 2012, 23:1-11.

[12] Bi Qingzhen, Huang Nuodi, Sun Chao, et al. Identification and compensation of geometric errors of rotary axes on five-axis machine by on-machine measurement. *Int J Mach Tools Manuf* 2015;89:182–91.

[13] Liang Xu, Yuchen Tian, Zhifeng Lou, et al. Error Analysis of a Kind of 3D Laser Ball Bar. *2019 The 4th International Conference on Design and Manufacturing Engineering* (2019) 012014 IOP Publishing doi:10.1088/1757-899X/627/1/012014

In this paper, a passive 3D laser tracking ball bar and the telescopic mechanism are proposed, and the error of the 3D laser tracking ball bar is analyzed, then the mathematical model of each error is listed. Furthermore, through numerical simulation, the influence degree of different errors on the device is obtained. The above research provides a new idea for the geometric error measurement of machine tools.